PHYSICAL REVIEW B VOLUME 30, NUMBER 1 1 JULY 1984

Positron diffusion in germanium

H. H. Jorch* and K. G. Lynn
Physics Department, Brookhaven National Laboratory, Upton, New York 11973

T. McMullen†
Physics Department, Memorial University of Newfoundland, St. John's, Newfoundland, Canada A1B 3X7

(Received 2 February 1984)

The temperature dependence of the diffusion constant of positrons in Ge single crystals is discussed. Experimental data on the fraction ($f_{\rm Ps}$) of 0–5-keV incident positrons reemitted from the surface as positronium are presented for Ge over the temperature range $300 \leq T \leq 1020$ K. The positron diffusion constant is deduced, at various temperatures, from an analysis using a one-dimensional diffusion model for $f_{\rm Ps}$ which is determined as a function of incident positron energy E. The magnitude and temperature dependence of the positron diffusion constant are compared with the predictions of the conventional weak carrier-phonon scattering theory that is used to describe the mobilities of electrons and holes in the elemental semiconductors. Conventional carrier-phonon scattering does not adequately represent the observed temperature dependence of the positron diffusion constant, and we investigate some possible origins of these discrepancies. Quantitative calculations identify several of these possibilities as implausible. We tentatively conclude that some form of positron-lattice coupling is the dominant interaction governing the positron motion.

I. INTRODUCTION

The naturally occurring charge carriers in the elemental semiconductors Ge, Si, and diamond are electrons and (heavy and light) holes. Measurement of the individual carriers' mobilities are somewhat more subtle than net conductivity measurements, since the conductivity results from a combination of the carrier mobilities and carrier densities. Nevertheless, the mobilities of electrons and holes in Si (Refs. 1 and 2) and Ge (Refs. 3 and 4), and of holes in diamond,[5] have been determined using carrier injection and time-of-flight techniques. These experiments require relatively low concentrations of thermally generated carriers and, as a consequence, mobility measurements on the naturally occurring carrier are, at present, restricted to temperatures $T < 300$ K. For this restricted temperature region there is good agreement[1–5] between experiment (on high-purity samples) and theory. The theory is based on the assumption of weak scattering of the carriers by the acoustic and optical phonons of the diamond-structure semiconductor lattice, and the scattering term in the Boltzmann equation is calculated by lowest-order perturbation theory. We shall refer to this theory as the conventional carrier-phonon scattering theory.

The study of the motion of a new positive-charge carrier, the positron, in the elemental semiconductors was initiated[6] by the drift-mobility measurements of Mills and Pfeiffer in Ge (Ref. 7) and Si (Ref. 8). With the advent of monoenergetic positron beams,[9] positron motional properties can be measured over a wide temperature range, including temperatures appreciably higher than those at which electrons or hole mobilities have been determined. Studies of this new carrier, with a simpler band structure than holes or electrons in the diamond-structure semiconductors, and with a wide temperature range available for mobility measurements, will enhance our understanding of the mobility-limiting processes in these materials.

The positron diffusion constant D_+ is related to the mobility μ_+ by the Einstein relation

$$\mu_+ = \beta e D_+ , \tag{1}$$

where $\beta^{-1} = k_B T$. In a positron-beam experiment, D_+ is found by determining the fraction of positrons implanted to depths ≈ 10–1000 Å which diffuse back to the surface within their lifetime of $\approx 2\times 10^{-10}$ s. The first extensive positron-beam measurements of positron diffusion in a semiconductor were those of Jorch *et al.*[10] in Ge over the temperature interval $300 \leq T \leq 1000$ K. Those results suggested the onset of a further mobility-limiting process at high temperatures, in addition to conventional carrier-phonon scattering.

In the present paper we present slow-positron-beam measurements of positron diffusion in Ge. In Sec. II we give a general discussion of measurements of positron motion in the near-surface region and of the analysis. The details of the Ge experiments are presented in Sec. III with a brief discussion of possible systematic errors associated with the experiments. In Sec. IV we extract the positron diffusion constants from the data and compare our results with the positron-mobility measurements of Mills and Pfeiffer,[7] as well as with the behavior of holes in this semiconductor. The predictions of conventional carrier-phonon scattering theory are also presented. In Sec. V we outline the current status of several theoretical ideas regarding carrier mobility which may be related to the origins of these discrepancies. In Sec. VI we present a summary and some concluding remarks.

©1984 The American Physical Society

II. INTERPRETATION OF SLOW-POSITRON-BEAM EXPERIMENTS

A. Positron thermalization

Monoenergetic positrons are typically produced by slowing high-energy (≈ 1 MeV) positrons emitted by a radioactive source with the use of a solid moderator. At present, various metals are used as moderators, and have efficiencies up to $\approx 10^{-3}$ emitted slow positrons per incident high-energy positron. The positrons emerge from the moderator with typically electron-volt energies, and most have only a thermal energy spread. They are then accelerated electrostatically and guided electrostatically and/or magnetically to strike a target surface of interest. Incident kinetic energies have varied from 10^0—10^4 eV, and beam currents are $\approx 10^{-13}$ A ($\approx 10^6$ positrons/s). Higher-energy beams, up to ≈ 100 keV, are now in operation.

Thermalization of high-energy positrons implanted into simple metals is reasonably well established both experimentally[11] and theoretically.[12] The experimental information indicates that most positrons reach thermal equilibrium with the lattice well within their lifetime down to temperatures <25 K. There is little direct experimental information[9] on thermalization from the kilo-electron-volt range, or on the important question of the shape of the positron-velocity distribution and the importance of nonthermal velocity trails at times of the order of the positron lifetime. Nieminen and Oliva[13] have carried out extensive calculations of slow-positron thermalization in Al and estimate thermalization times of ≈ 7 ps to 300 K and ≈ 60 ps to 15 K. There has been little investigation of the details of thermalization in semiconductors, where electron-hole—pair excitation is forbidden for e^+ kinetic energies less than the band gap. In Appendix A we present an estimate of the energy-loss rate in Ge and Si. This estimate suggests that thermalization is nearly complete down to the sample temperatures used here, and our interpretation of the experiment proceeds on that assumption. Shulman *et al.*[14] have reported evidence of positron thermalization to <80 K in Ge.

As positrons of incident kinetic energy E slow within the sample, they can be characterized by their depths $x \geq 0$ below the surface and velocities $\vec{v}$ at a time t after entering the solid, and described by a distribution function $p(x,\vec{v},t \mid E)$. The spatial resolution of this semiclassical distribution is the positron wavelength, which at 300 K is $\simeq 100$ Å. Some positrons are initially reflected, and others escape through the surface as time progresses, and thus

$$\int_0^\infty dx \int d^3v\, p(x,\vec{v},t \mid E) < 1 \tag{2}$$

gives the fraction remaining within the solid at time t. The positron thermalization time $t_{\rm th}$ is defined as the earliest time at which

$$p(\vec{v},t \mid E) \equiv \int dx\, p(x,\vec{v},t \mid E) \tag{3}$$

is essentially indistinguishable from the thermal equilibrium distribution in the solid (which is not necessarily Boltzmann[15,16]) in an experiment. If the thermalization time is short compared to both the positron lifetime and the diffusion time back to the surface, the stopping profile[9,17]

$$p(x \mid E) \equiv \int d^3v\, p(x,\vec{v},t_{\rm th} \mid E) \tag{4}$$

is a reasonably well-defined and useful quantity. The positron scatters through large angles as it slows, so by $t_{\rm th}$ the direction of $\vec{v}$ will be nearly random. We will assume in the following analysis that $t_{\rm th}$ is short and that $p(x \mid E)$ is well defined.

The stopping profiles of positrons in solids are not yet very well known, although some measurements[9,18] have been made. The mean depth $\bar{x}$ appears to increase roughly as E^n with a proportionality constant $\approx 10^2$ Å/keV^n, and exponent $n \simeq 1.6$. The stopping profile enters the analysis as an initial condition in the solution of the diffusion equation which describes the subsequent time and space evolution of the positron distribution. In Sec. II C we shall suppose the profile to be exponential,[19,20] and in Sec. II D we present some evidence that the results are primarily sensitive to first moment $\bar{x}$ of the profile and not to details of the true profile shape.

B. Surface processes

Following thermalization, the positron motion is diffusive on a length scale much greater than the mean free path (which is ≈ 10 Å at 300 K and varies as T^{-1} for positron-phonon scattering). Since the positron can return to the surface before annihilation, either prior to thermalization or with thermal energies via diffusion, it may encounter any of several experimentally observed fates, which are the following (Fig. 1):

(i) annihilation from a bulk (or defect-localized) state within the material;

(ii) trapping in a two-dimensional (or defect-localized) positron surface state[21] followed by either (a) annihilation from that state, or (b) thermal desorption from the surface state as positronium (Ps);[22]

(iii) direct emission as Ps (Refs. 23 and 19) or Ps$^-$ (Ref. 24);

(iv) direct reemission as a free positron.[25]

The direct reemission processes (iii) and (iv) are only possible for thermal positrons if the work function is negative for positrons, Ps or Ps$^-$.

In these positronium emission studies, a small bias is applied which returns essentially all the reemitted slow positrons to the surface. The surface then behaves somewhat as an internal reflector of positrons. Energy losses are known to occur[26] as positrons pass through the surface region, so the reflection is not totally elastic. This reflection presumably produces a distortion of $p(x \mid E)$, increasing p for very small x, the magnitude of which is difficult to assess and should be sample dependent. The inelasticity of reflection may enhance surface-state trapping. In the present experiments, all positrons reemitted were returned back to the sample by the biasing arrangement.

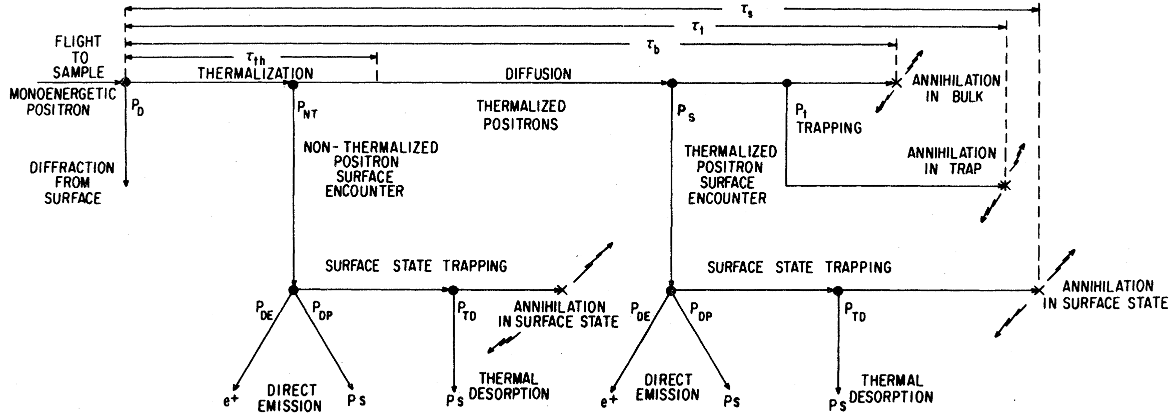

FIG. 1. Predominant possible fates of the monoenergetic positron involving a solid. Some minor branches such as formation of Ps^- and prethermalized trapping have been omitted for clarity. The time scale is depicted as increasing montonically to the right but is not proportionally correct. Branching ratios are marked as P_i and mean times as τ_i.

C. Separation of surface processes from bulk diffusion

At average times greater than t_{th} and on sufficiently long length scales the positron motion is diffusive, and the following model assumes diffusive motion. It is thus limited to positrons implanted at depths of several mean free paths or wavelengths, and is expected to be inapplicable at very low implant energies or sample temperatures. In Fig. 1 the probability that a positron escapes from the sample prior to thermalization is denoted P_{NT}. The work of Mills and Platzman[27] on Cu and Al indicates that the probability P_D of positrons being elastically backscattered is small ($<1\%$) for $E>20$ eV. The probability P_B of annihilation in bulk depends on the likelihood of the thermalized positron returning to the surface before annihilation or trapping in a defect. Nieminen and Oliva[13] present one of the more complete discussions of the diffusion model for this process. We let

$$F \equiv (P_{\text{th}} - P_B)/P_{\text{th}} \tag{5}$$

be the fraction of thermalized positrons which meet one of the possible fates involving the surface ($P_t=0$). This fraction is calculated from the solution of the diffusion equation

$$\frac{dn}{dt} = D_+ \nabla^2 n - \frac{n}{\tau} , \tag{6}$$

where $n(\vec{r},t)$ is the thermalized-positron spatial distribution, t is measured from the thermalization time, and τ^{-1} is the effective annihilation rate in the bulk sample. If an internal electric field $\vec{\varepsilon}$ is present in the sample, which is a possibility in some materials such as Ge and Si, an additional term $\beta e D_+ \nabla \cdot (\vec{\varepsilon} n)$ appears in (5).[28] This term will not be explicitly included in the analysis here, for the magnitude of any such field in the present experiments is unknown. Its possible influence on the extracted diffusion constants is discussed in Sec. V.

The diffusion equation is solved in one dimension with the initial condition

$$n(x, t=0) \equiv n_0(x) = p(x \mid E) \Big/ \int_0^\infty dx\, p(x \mid E) . \tag{7}$$

The spatial boundary condition is

$$D_+ \frac{\partial n}{\partial x}\bigg|_{x=0} = \nu n \bigg|_{x=0} , \tag{8}$$

which states that the positron flux toward the surface must be equal to the rate of disappearance of positrons at the surface, with the latter assumed to be proportional to the positron density $n(x)$ at the surface. The proportionality constant ν includes both the direct escape processes through the surface and trapping in the surface state. Thus, $\nu n(x=0)$ gives the number of positrons that pass into the surface per unit area per unit time to meet one of these fates.

The diffusion length

$$L_+ = (D_+ \tau)^{1/2} \tag{9}$$

estimates an average distance that a positron can diffuse in the bulk solid during its lifetime. The distance $\nu\tau$ is a measure of the rate at which surface processes remove positrons from the bulk solid, and is roughly the depth over which a unit positron density could potentially be depleted by surface processes during the bulk positron lifetime. In terms of these two lengths, the solution to (6)—(8) gives[13,19,29]

$$F = \tilde{n}_0(L_+^{-1})/(1+L_+/\nu\tau) , \tag{10}$$

where

$$\tilde{n}_0(\alpha) = \int_0^\infty dx\, n_0(x) e^{-\alpha x} \tag{11}$$

is the Laplace transform of the normalized positron stopping profile (7). Thus, the significant region of the stopping profile is $0 < x \lesssim L_+$. If $\nu\tau \gg L_+$, nearly all positrons which reach the surface are removed through surface processes. If $\nu\tau \ll L_+$, then most positrons which reach the surface are reflected back into the interior of the sample.

In the experiments presented here, it is not the fraction F which is measured, but the fraction f_{Ps} of positrons which escape as positronium and decay in vacuum. The way in which the characteristic Ps annihilation signal is

separated from that of positron annihilation is described in Sec. II F. The Ps which originates from thermalized positrons emerges from the sample with kinetic energies <5 eV, i.e., velocities $<10^6$ m/s, so singlet Ps travels at most a few millimeters before annihilating. The longer-lived triplet Ps can travel distances ≈ 10 cm prior to annihilation, and care must be taken to minimize pick-off annihilation of the triplet Ps due to collisions with the experimental hardware, and to reduce errors resulting from the decreased solid angle subtended by the detector. However, the pick-off probability or trapping into the surface state due to collisions is unknown since the Ps reflection coefficient at these energies is not known.

The total rate of surface processes can be decomposed into rates for the individual processes

$$\nu = \nu_{e^+} + \nu_{\mathrm{Ps}} + \nu_{\mathrm{Ps}^-} + \nu_s \ , \tag{12}$$

where the first three terms give the direct emission rates for the three species and ν_s is the net transition rate into the positron surface states. The ν_{Ps^-} term will be ignored since the Ps^- formation rate is well below the values of the other terms in the present experiments and energetically unfavorable in most systems. Of those positrons trapped in the surface states, a fraction P_{TD} can be thermally desorbed as Ps, so the fraction of initially thermalized positrons which are emitted as Ps is

$$f_{\mathrm{Ps}}(E,T) = \left[\frac{\nu_{\mathrm{Ps}} + \nu_s P_{\mathrm{TD}}}{\nu} \right] F \equiv f^0_{\mathrm{Ps}} \tilde{n}_0(L_+^{-1}) \ . \tag{13}$$

In experiments such as those presented here, the biasing fields return all reemitted positrons to the surface. Those not experiencing inelastic processes on traversing the surface are returned to the bulk, while those which do are trapped in the surface state (or possibly emitted as Ps) and included in ν_s (or ν_{Ps}). Hence $\nu_{e^+}=0$ here.

The various escape rates ν_i and the diffusion length L_+ change with sample temperature. However, if the temperature is held constant and the incident-positron energy E is varied, only the Laplace transform ($\tilde{n}_0$) of the implantation profile (n_0) changes if the positrons are thermalized. If we suppose that the general shape of n_0 remains unchanged and that L_+ is independent of E and assume, for example, an exponential profile of the form $\bar{x}^{-1}\exp(-x/\bar{x})$, then

$$\tilde{n}_0(L_+^{-1}) = \frac{1}{1+\bar{x}/L_+} \tag{14}$$

depends on E only through the mean implantation depth $\bar{x}$. Varying $\bar{x}$ by varying E at constant temperature allows one to establish the dependence of $\tilde{n}_0$ on E, and this is what is done in the experiments. The exponential form (14), which is believed at present to be a reasonable (although see Ref. 18) as well as convenient representation of the profile, is the form used in the present analysis for this restricted energy range ($E \leq 5$ keV).

To proceed further in the analysis, a relationship between the mean implanation depth ($\bar{x}$) and the incident-positron energy (E) must be established. Fits of experimental data to (13), and to the corresponding expression for the slow-positron yield, using the exponential profile for $p(x \mid E)$, suggest[30] that, as discussed in Sec. II A,

$$\bar{x} = AE^n \ , \tag{15}$$

where $1 < n < 2$.

With a specific form for n_0 and $\bar{x}$ expressed in terms of the measured quantity E, the diffusion length L_+ and the diffusion constant D_+ [from L_+ and τ, using Eq. (9)] can be determined. Since there appears to be no reason to anticipate a dependence of the $\{\nu_i\}$ on $\bar{x}$, in practice one uses the known limits

$$\lim_{\bar{x}\to 0} \tilde{n}_0 = 1 \quad \text{and} \quad \lim_{\bar{x}\to\infty} \tilde{n}_0 = 0 \ ,$$

together with measured values of $f_{\mathrm{Ps}}(E)$, and fits the assumed $\tilde{n}_0$ expression to the data to extract L_+ (Fig. 2). It is important to have sufficient energy to reach an x which is several times L_+ at any given temperature to check for symptoms of a poor choice of the assumed n_0.

One must be cautious in interpreting data near the $\bar{x}=0$ limit because of the inadequacy of the diffusion model at the short distances mentioned above. This analysis is independent of the temperature dependence of the escape rates $\{\nu_i\}$ since each determination of L_+ is at a fixed temperature.

D. Positron stopping profiles

Although bulk positron lifetimes τ_B have been accurately measured, positron stopping profiles are not yet well known. Mills and Wilson[18] have recently reported the first approximate measurement of $p(x \mid E)$. They determined the positron transmission coefficient η as a function of film thickness x using thin films of Al and Cu. They find $\bar{x} \propto E^n$ with $n=1.6$ in Al, in agreement with the earlier result of Lynn and Lutz[30] who fitted f_{Ps} to (13) and (14). Their measured approximate stopping profiles $-\partial\eta/\partial x$ are not well described by the exponential approximation, however. Instead, for both Cu and Al,

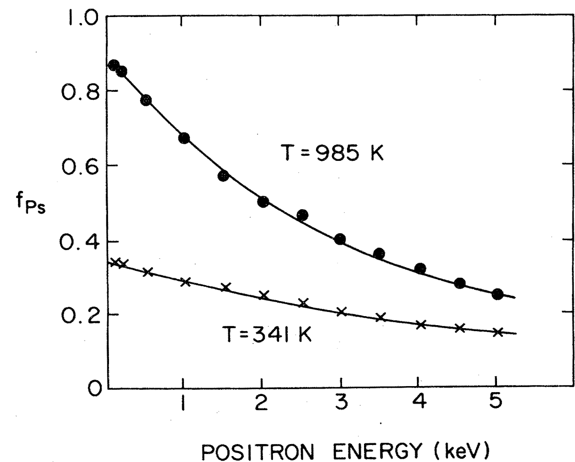

FIG. 2. Example of positronium fraction data (f_{Ps} versus incident-positron energy E) for Ge(110) at different temperatures. The solid curves are fits of (13) using the exponential implantation profile expression (14).

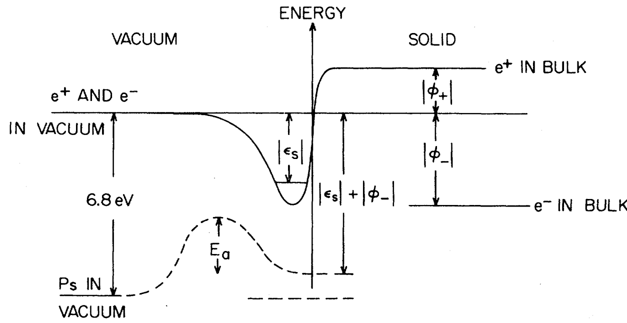

FIG. 3. Energies involved in Ps thermal desorption. ϵ_s is the ground-state binding energy in the surface state, ϕ_- is the electron work function, and 6.8 eV is the binding energy of positronium.

$-\partial\eta/\partial x$ peaks some distance below the surface, and cuts off fairly abruptly at a maximum range which increases with energy. They estimate the backscattering correction, i.e., the difference between $p(x\mid E)$ and $-\partial\eta/\partial x$, to be small. However, this backscattering fraction will affect the overall shape of the stopping profile, making it more like an exponential profile. It is difficult to assess the error introduced in the Ge and Si positron diffusion constants of Sec. IV by our use of the exponential approximation. Valkealahti and Nieminen[31] employ a Monte Carlo simulation technique for determining ranges in solids and conclude that D_+ could be in error by up to 20% by assuming the incorrect profile. We note, however, that the good agreement of the exponential profile approximation with the data shown in Fig. 2 is typical. Jorch,[29] who investigated the sensitivity of the analysis to the shape of profile used, found that L_+ was not significantly affected by the detailed shape and concluded that the mean penetration depth $\bar{x}$ is the most important parameter. Tests comparing the analysis of the Ge data using an exponential, δ function, and modified-Gaussian profile show large differences in the energy parameter E_0 [see Eq. (17)] and exponent n. Differences in L_+ (between the three profiles) were all well within error limits, however, indicating that the fitting procedure uses the weakly defined parameter n to compensate for inadequacies in the model. This results in a value for L_+ which is only weakly dependent on the shape of the profile chosen for the analysis.

Mills and Wilson[18] find that the positron mean pentration depth $x_{1/2}$ for their films of Al, Cu, and Si is well represented for $E<5$ keV by $x_{1/2}=aE^n$ with $a=3.3$ $\mu\mathrm{g\,cm^{-2}\,keV^{-n}}$ and $n=1.6$, for E in kilo-electron-volts. For the exponential profile, $A=a/\rho\ln 2$ where ρ is the mass density, and this gives the A values for Ge and Si which appear in Table I and are used to obtain the diffusion constants in Sec. IV.

TABLE I. Positron penetration-depth coefficient in $\bar{x}=AE^n$.

	a (μg/cm^2)[a]	ρ (g/cm^3)	A (Å keV^{-n})
Ge	3.32	5.36	89
Si	3.32	2.33	206

[a]Reference 18.

E. Positronium emission processes

Positronium emission from surfaces is believed to arise from two different physical processes, an essentially temperature-independent process and a thermally activated process with an activation energy of ≈ 0.5 eV.[9] The former is interpreted as direct emission of Ps and the latter as thermal desorption of a positron from a surface state, both requiring capture of an electron from the solid during escape. The energies that would then be involved are shown in Fig. 3. For such light particles, quantum effects such as barrier penetration may play a significant role.

At low implant energies ($E<0.1$ keV) where diffusion to the surface is not a limiting factor, and with biasing fields to prevent positron reemission, it appears that (at high temperatures) essentially all thermalized positrons are emitted as positronium from a number of surfaces (e.g., $>90\%$ from Al, Ag, and Cu surfaces above 800 K). This was established[20] by using an intrinsic Ge detector, as described in Sec. II F, to measure the ratio of three-photon positronium annihilations to total annihilations detected by the spectrometer system. The detector was located either behind or beside the sample and annihilations both within and in front of the sample were counted. There is no evidence for positronium in the interior of an elemental semiconductor or a metal, but with this procedure we are unable to distinguish between adsorbed Ps and Ps in vacuum. It seems highly unlikely, however, that Ps with its unpaired electron can exist as an entity adsorbed on a semiconductor surface, and the adsorbed species is presumably a positron trapped in a surface state.

At low implant energies the thermally activated positronium emission process accounts for 30–50% of the positronium emission from Ag and Cu surfaces at high temperatures.[20] The apparently temperature-independent process contributes the remaining fraction. Slow-positron emission also occurs from *unbiased* surfaces. The fraction of incident positrons f_{e+} which are reemitted as slow positrons (frequently called the slow-positron yield y_+) is ≈ 0.1 for clean Al, Cu, and Ge surfaces.[25,29,30] There is as yet no evidence of a thermally activated process for slow-positron emission, i.e., positrons trapped in the surface apparently desorb exclusively as Ps.

F. Positronium detection

The detection of Ps in these experiments relies on the fact that, for triplet Ps in vacuum, two-photon annihilation is forbidden and three-photon decay is the dominant annihilation mechanism. In contrast, singlet Ps and positron annihilation in condensed matter predominantly produce two photons, each of which is required by energy-momentum conservation to have an energy of ≈ 511 keV. Consequently, the ratio (P/T) of the number (P) of photons detected in the 511-keV "photopeak" to the total number (T) of annihilation photons is used to obtain the fraction of implanted positrons which escape and form Ps. Three conditions must be met for the analysis to be valid. The triplet-to-singlet Ps-state population ratio is assumed to be independent of the experimental parameters (incident energy and sample temperature). Ps must exist

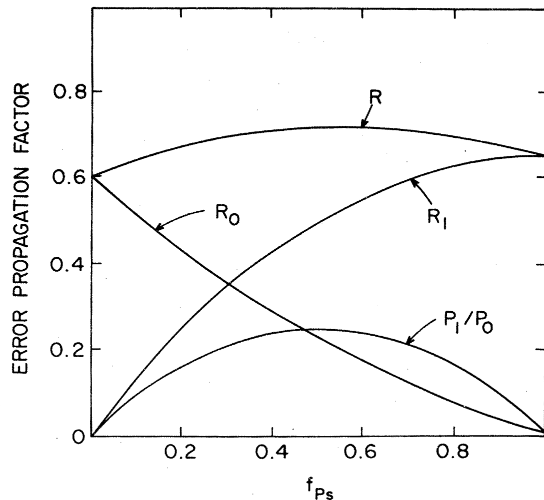

FIG. 4. Propagation of relative errors in the variables of (16) to the positronium fraction f_{Ps}, for a representative value of $P_1/P_0=0.5$. In every case, the error is reduced in propagation, e.g., a 1% error in R will produce, at most, a 0.7% error in f_{Ps}.

only outside the sample and decay in vacuum; otherwise, some of the triplet positronium could annihilate (due to pickoff) by the two-photon mode. Thirdly, neither positrons nor Ps should escape from the region examined by the detector, and the experimental geometry is arranged to minimize this escape.

In practice, the ratio $R=(T-P)/P$ is used and must be established for a given experimental system, in the two limits of 0% and 100% Ps formation. Determining either limit is not straightforward at present. The 0% limit R_0 involves implanting positrons so far into a metal, where Ps cannot form, that none can diffuse back to the surface in their lifetime. This is usually done with a metal which contains defects (traps) produced by ion sputtering. Determination of the 100% limit R_1 involves a further difficulty—one requires a sample which converts 100% of emitted positrons to Ps. Since evidence has accumulated that at low implant energies and high temperatures some surfaces, e.g., Al, emit essentially all implanted positrons as Ps, these surfaces are used to establish R_1. Experience leads us to believe that, on the Brookhaven system, we have the capability to determine, on an absolute scale, $f_{Ps}=(0\pm5)\%$ and $f_{ps}=(100\pm5)\%$ in the two limits. However, confirmation of these estimates is needed and awaits further experimental development.

Since, in the 100% Ps case, there are contributions to the counts P in the photopeak region, the ratio of the two limits P_1/P_0 also enters the expression[19,20]

$$f_{Ps}=\left[1+\left[\frac{P_1}{P_0}\right]\frac{R_1-R}{R-R_0}\right]^{-1}, \tag{16}$$

which gives the Ps fraction experimentally for arbitrary R. The errors propagated in the determination of f_{Ps} from errors in the measured values of P and T and in the limits have been investigated by Jorch.[29] One example is shown in Fig. 4, where for a typical value of P_1/P_0, the ratio of the relative uncertainty $\delta f_{Ps}/f_{Ps}$ induced in f_{Ps} to the relative error $\delta m/m$ in a measured quantity m is plotted. The contribution to the relative uncertainty in f_{Ps} is less than or of the order of $\delta m/m$ for all reasonable values.

G. Summary of the state of the art

The types of experiments described above are becoming a useful probe of the surface and near-surface region of solids. In the near-surface region, the difffusing positrons can probe open-volume defect structures in addition to permitting studies of the motion of a positive charge carrier such as those to be presented here. The nature of the surface is studied by measuring the emission properties of positrons and of positronium. The techniques are still evolving, and probably the most serious uncertainty in positron diffusion measurements, at present, arises from our lack of information about the implantation profile. The calibration difficulties mentioned in Sec. II F are less significant for diffusion studies, which probe L_+, than for surface studies, which probe $\{\nu_i\}$.

III. EXPERIMENTAL SETUP

The samples used were single crystals cut and polished so that the surface presented to the positron beam was within $\sim\pm1°$ of a low-index crystal axis as determined by the Laue x-ray backscattering pattern. Before insertion in the UHV system of the positron-beam apparatus,[32,33] each sample was etched in a HNO_3-HF mixture, washed in alcohol, and dried in air. Several cycles of high-temperature annealing and sputtering with Ar were performed *in situ*. The Ar ions bombarded the sample at glancing incidence ($\approx 20°$). Initially, ion energies of 1—2 keV were used to remove the native oxide, and then sputtering was done at energies of a few hundred electron volts in an attempt to minimize defects generated by the ion bombardment. Annealing was limited to temperatures near 1000 K since above this temperature range the vapor pressure of Ge becomes a problem and vacuum components in line of sight of the sample become coated with the sample material.

The amount of surface contamination was monitored by Auger-electron spectroscopy (AES) and near-surface crystalline perfection was occasionally checked by low-energy electron diffraction (LEED). Crystalline perfection of the surface in the annealing stages was determined using the Ps emission fraction as a final criterion, not the attainment of a particular LEED pattern.

The Ge(111) and Ge(100) crystals were cut from hyperpure material used in solid-state photon-detector fabrication and obtained from the Space Products Division of General Electric. The (111) material was In-doped at $<10^{14}$ cm^{-3} with a resistivity of ≈ 1 Ω cm and the (100) was Ga-doped at $<10^{14}$ cm^{-3} with a resistivity of ≈ 30 Ω cm. Both had dislocation densities below 10^3 cm^{-2}, active impurity levels (donor acceptor) below 10^{11} cm^{-3}, and other impurities below $\approx 10^{14}$ cm^{-3}. The Ge(110) crystal was cut from material used for neutron monochromator purposes. Impurity levels are estimated to be below 10^{18} cm^{-3} and the crystal used has a resistivity of ≈ 400 Ω cm.

Sample temperatures were measured with a W-RE thermocouple in contact with the sample. The incident-positron energy was chosen by a suitable biasing of the sample stage and accelerator tube.[32] A small potential difference between the sample stage and accelerator served to ensure that emitted positrons were attracted back to the sample, i.e., only Ps could escape into the vacuum.

IV. POSITRON DIFFUSION CONSTANTS

A. Method of determining D

In the experimental profile model the incident-positron energy E_0 at which the positronium fraction $f_{\rm Ps}(E,T)$ falls to $\frac{1}{2}$ of its $E\rightarrow 0$ value can be related to the diffusion length by

$$L_+ = AE_0^n = \bar{x}(E=E_0) \tag{17}$$

from (14) and (15). The diffusion constant of positrons in Ge obtained from

$$D_+ = L_+^2/\tau = (AE_0^n)^2/\tau \tag{18}$$

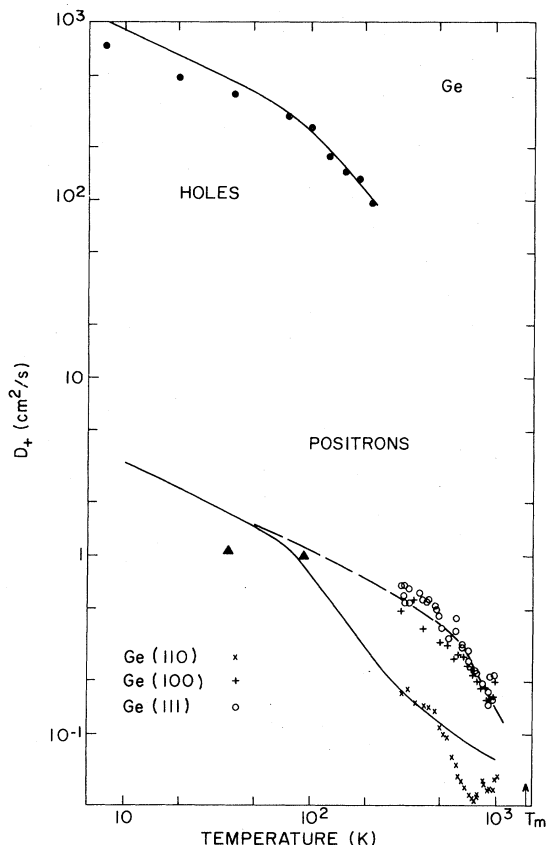

FIG. 5. Diffusion constant of positrons in Ge. Comparison of the present results with those of Mills and Pfeiffer (Ref. 7) (triangles), with conventional carrier-phonon scattering theory using $E_1=20$ eV and $E_1^{\rm opt}=40$ eV (solid curve), and with the diffusion constant for holes (Ref. 4) (dots). Also shown is a fit of the simple carrier-phonon scattering theory discussed here to the hole diffusion constant data, using $E_1=4.5$ eV and $E_1^{\rm opt}=6.5$ eV. Our D_+ was calculated with $A=89$ Å keV^{-n}, $\tau=227+0.01T$ ps, and $n=1.4$, using (18). The "theory" responsible for the dashed curve is described in Sec. V E.

is shown in Fig. 5, and the A value used is given in Table I. An expression for the positron bulk lifetime in Ge,

$$\tau = 227+0.01T \text{ ps} , \tag{19}$$

was constructed using the bulk lifetime of 230 ps (Ref. 34) at room temperature and a linear interpolation of the reported[35] increase $\Delta\tau=7$ ps upon increasing the temperature from 300 to 1000 K. Equation (18), as presented, assumes that no trapping sites for positrons are present in the crystal, although this can be easily modified by including a trapping-rate term in τ (see Sec. V F). The exponent value $n=1.4$ was used throughout, consistent with recent measurements[18] which give $n=1.4$ for Cu, which is close to Ge in the Periodic Table. This n value is within the estimated uncertainty of ± 0.1 of the slightly varying values produced by the fitting routine for the individual sets of $f_{\rm ps}$-versus-E data.[36] The diffusion constant of Mills and Pfeiffer,[7] obtained from their low-temperature positron-mobility data through the Einstein relation (1), is also shown in Fig. 5.

B. Germanium

In Fig. 5 we also show the diffusion constant for holes in Ge, obtained from the mobility data of Reggiani *et al.*[4] The hole mobility, not the electron mobility, is the closer analog to the positron mobility. Positrons and holes are both positively charged, but the more important reason is the simpler band structure of holes compared to electrons. The holes occupy the Brillouin-zone center, while the electrons occupy eight ellipsoidal valleys at the zone boundary in the [111] directions and exhibit anisotropic effective masses and intervalley scattering. At low temperatures the hole diffusion constant varies with temperature as

$$D \propto T^{-\xi} , \tag{20}$$

where $\xi \simeq 0.3$. Conventional acoustic-phonon scattering predicts $\xi=0.5$ for a single parabolic band. The holes, however, occupy both the heavy- and light-hole bands. At temperatures above 100 K the slope $\partial \ln D/\partial \ln T \equiv -\xi$ for Ge holes is observed to steepen due to the onset of optical-phonon scattering.[4]

For comparison with the positron-diffusion-constant measurements we consider the simplest model of a carrier undergoing conventional weak scattering from bulk acoustic and optical phonons. Ge and Si have cubic symmetry, so mobility and diffusion exhibit no anisotropy. For an isotropic parabolic band $\epsilon_k=\hbar^2k^2/2m^*$ we have

$$D = \frac{\hbar^2}{3m^{*2}} \langle k^2 \tau_k \rangle , \tag{21}$$

where τ_k is the momentum relaxation time. Scattering of the carrier from acoustic phonons is nearly elastic and scattering from optical phonons is velocity randomizing, so a relaxation time exists for both processes. Treating the scattering from longitudinal-acoustic (LA) phonons in a deformation model gives a relaxation-rate contribution

$$(\tau_k^{\rm LA})^{-1} = \frac{1}{\pi} E_1^2 \frac{m^* k}{\beta \hbar^3 \rho s^2} , \tag{22}$$

where E_1 is the deformation-potential constant, ρ is the mass density, and s is the sound velocity. Thus, performing the average $\langle\ \rangle$ over the Boltzmann distribution gives $D \propto T^{-1/2}$. Some authors use slightly different definitions of the acoustic-phonon deformation-potential constant; our definition E_1 is that used for positrons by Mills and Pfeiffer.[7]

Scattering from longitudinal-optical (LO) phonons of frequency ω_0 can also be treated in a deformation-potential model. The deformation-potential constant $E_1^{\rm opt}$ is chosen so that the expressions for the LA and LO phonons are formally identical. When this is done, it is the quantity $\omega_0 E_1^{\rm opt}/2s$ which gives the carrier energy shift per unit increase in separation of a pair of atoms within the unit cell.[37] The momentum relaxation rate is

$$(\tau_k^{\rm LO})^{-1} = \frac{1}{2\pi}(E_1^{\rm opt})^2 \frac{\omega_0 m^* k}{\hbar^2 \rho s^2}\left[\frac{(1+\hbar\omega_0/\epsilon_k)^{1/2}}{e^{\beta\hbar\omega_0}-1} + \frac{(1-\hbar\omega_0/\epsilon_k)^{1/2}}{1-e^{-\beta\hbar\omega_0}}\Theta(\epsilon_k - \hbar\omega_0)\right], \tag{23}$$

where the step function Θ only permits optical-phonon emission when $\epsilon_k > \hbar\omega_0$.

Substitution of $\tau_k^{-1} = (\tau_k^{\rm LA})^{-1} + (\tau_k^{\rm LO})^{-1}$ in (21) gives the expression for the diffusion constant[38,39] which is compared with the Ge hole mobility in Fig. 5. For Ge holes, an effective mass $m^* = 0.35 m_e$, where m_e is the free-electron mass, has been used.[4] The values of $E_1 = 4.5$ eV and $E_1^{\rm opt} = 6.5$ eV used in calculating the theoretical curve shown are similar to the values in the more sophisticated model of Reggiani *et al.*[4] The optical-phonon temperature $T_{\rm op} \equiv \hbar\omega_0/k_B = 430$ K of Ge reproduces the steepening of the slope of the experimental data[4] at $T \simeq 100$ K satisfactorily, although the theoretical value of $\xi = 0.5$ appears somewhat too large at low temperatures.

The positron diffusion data in Fig. 5 shows several features not shared by the data for holes. The positron data extend to appreciably higher temperatures than that for holes. Regrettably, it has not yet been possible to reliably extend the slow-positron-beam data to temperatures below 300 K because of technical problems. The experimental difficulties preventing this are twofold. We have found it necessary to thoroughly anneal Ge at high temperatures in order to produce consistent results, and our present low-temperature ($30 < T < 300$ K) sample manipulator does not permit this. Secondly, when the sample manipulator is changed it is necessary to recalibrate the limiting P and R values for positronium detection, and the uncertainty in the calibration for two different geometries is signficantly greater than for a single geometry at different temperatures. When these experimental problems are overcome, measurements spanning the entire temperature range will not only establish unambiguously the absolute values of D_+, but will permit comparison of the beam measurements with the drift-mobility measurements of Mills and Pfeiffer[7] and hence an independent check on the A values of Table I.

The $D_+(T)$ results for diffusion in the three different planes (100), (110), and (111), normal to the surfaces of the three different samples should, in principle, be identical for impurity- and defect-free Ge. One possible explanation for the lower values of D_+ along (110) is that the penetration depth is orientation dependent.[10] It is interesting that the (110) plane has the largest open channels in the diamond structure. Owing to the present uncertainty in and possible orientation dependence of A, the absolute position of each set of data on the vertical axis is somewhat uncertain.

Nevertheless, the dependence on the temperature in each set of data is, as discussed in Secs. II and III, reliable. The low-temperature points of Mills and Pfeiffer[7] suggest a temperature dependence ξ which appears to be less than that for Ge holes, and their original measurements are not consistent with ξ as large as 0.5 for $T < 100$ K. Our measurements at $T < 400$ K also suggest a lower value of ξ, although because of the limited temperature range the uncertainty is large. Furthermore, our (110) and (111) measurements at $T < 400$ K agree in magnitude with those of Mills and Pfeiffer if a low-slope region $\xi < 0.5$ continues out to 400 K. At $T \approx 500$ K there is a clear indication of an increase to $\xi \approx 1.6$ for (100) and (111) and as much as $\xi \approx 2.1$ for (110).[40] Above 800 K there is a further change in the temperature dependence. The slope ξ is reduced considerably, with $D_+(T)$ becoming essentially temperature independent and with even an indication of an increase in D_+ at $T \approx 1000$ K. Beyond 1000 K, however, it appears that the decline in D_+ resumes. (The melting point of Ge is 1211 K.)

The solid curve show the behavior of the positron as predicted by conventional carrier-phonon scattering theory. For the positron, we have taken $m^* = m_e$, consistent with the measurements of Shulman *et al.*[14] Since $D \propto m^{*-5/2}$, the mass difference between the positron and the hole accounts for a reduction $D_+/D_h \simeq 0.072$ in the theoretical curve which is compared with the positron data. The remainder comes from the increase in deformation-potential coupling constants used for the positron, which are $E_1 = 20$ eV and $E_1^{\rm opt} = 40$ eV. The value of E_1 was chosen to place the theoretical curve roughly in agreement with the measurements of Mills and Pfeiffer, and is close to their extracted value of $E_1 \simeq 19$ eV.[7] The $E_1^{\rm opt}/E_1$ ratio is higher than that used for holes to give a slope in the $T \gtrsim 500$ K range similar to that of the data. However, for all choices of E_1 and $E_1^{\rm opt}$ the slope change in the theoretical curve remains near 100 K due to the fixed optical-phonon temperature ($T_{\rm op}$) which determines the onset of the scattering as given by (23). At $T \gg T_{\rm op}$, optical-phonon scattering saturates and the slope $\partial \ln D / \partial \ln T$ of the theoretical curve again returns to the characteristic acoustic-phonon slope of $-\frac{1}{2}$. The limitation on the wave vector $\vec{q}$ of the acoustic phonons which participate is $\vec{q} < 2\vec{k}$, and since the positron thermal wave vectors are small even at the highest temperatures, neither acoustic-phonon saturation nor umklapp scattering modify (22) significantly.

There are several striking disagreements between the experimental results and conventional carrier-phonon scattering theory. Although the data of Mills and Pfeiffer are consistent with the theory, the present (110) data, in

particular, suggest a continuation of $\xi \approx 0.5$ up to 500 K, where the curve steepens. With sufficiently strong optical-phonon coupling, the *slope* in the (500—900)-K region can be reproduced by the theory, but the *slope change* is predicted to occur near 100 K instead. We are forced to conclude that conventional weak carrier-phonon scattering theory does not adequately account for the experimental results on positron diffusion in Ge.

V. SPECULATIONS ON POSITRON MOTION IN Ge

We have no consistent explanation for the observed behavior of D_+ in Ge at present. In this section we examine various ideas concerning carrier motion and identify some which quantitative estimates suggest are not relevant.

A. Positron-electron and positron-hole scattering

Semiconductors contain thermally generated electron-hole pairs, and the density of these carriers increases as $T^{3/2}\exp(-\beta E_g/2)$, where E_g is the band gap, in an intrinsic semiconductor. It is of interest to see if the rapid decrease in D_+ for Ge above 500 K could be due to scattering from thermally generated carriers taking over from acoustic-phonon scattering as the dominant scattering mechanism at $T \simeq 500$ K.

We estimate D_+ for scattering from thermally generated carriers as follows. Consider positrons of mass $m^* = m_e$ interacting with electrons and holes of mass $m^* = m_e$ in an isotropic parabolic band. The Coulomb potential is screened over distances on the order of Debye shielding length q_D^{-1} where

$$q_D^2 = 4\pi\beta e^2 n_c/\epsilon \ , \qquad (24)$$

with n_c the carrier density and ϵ the dielectric constant ($\epsilon = 16$ for Ge). Use of this screened potential allows us to calculate the relaxation rate τ_k^{-1} in the elastic scattering approximation, valid when q_D is small compared to thermal wave vectors. The details of the calculation are given in Appendix B. We find, in the steps leading to the expression for τ_k^{-1}, that the increase in the number of carriers n_c from which the positron can scatter is compensated by the decrease in the range q_D^{-1} of the screened potential. The increase in available phase space leads to a fairly strong decrease in D_+ with increasing temperature, corresponding to $\xi \simeq 4$–5 at $500 < T < 1000$ K in Ge. However, D_+ for positron-carrier scattering in this approximation always remains small compared to D_+ for positron-phonon scattering, and shows a tendency to saturation for $1000 < T < 1200$ K at a value $D_+ \simeq 50$ cm^2/s. This dominance of positron-phonon scattering over positron-electron scattering is also found for metals[41] where the density of electrons is large. Positron experiments which sample the interior have shown no sensitivity to the large changes in carrier concentration from 5 to 300 K (Ref. 14) and from 350 to 1100 K (Ref. 42) in Ge and between 77 and 300 K in Si (Refs. 42 and 43). Various degrees of doping giving a range of resistivity from intrinsic material to 10^{-2} Ω cm have produced no changes in the positron's behavior in Si (Refs. 42—44) and no effect was found to 10^{-4} Ω cm in Ge (Ref. 14).

Consequently we conclude that even if band bending produces a higher electron density near the surface than in bulk, positron-carrier scattering is an unlikely explanation of the decrease in D_+ observed in Ge above 500 K. We have not thoroughly investigated the possibility of formation of a positron-carrier excitonlike complex, but the required cross sections and binding energies seem too large.

B. Positron scattering from impurities and defects

The momentum relaxation rate for scattering from singly ionized impurities is[38]

$$\tau_k^{-1} = \frac{\pi n_I \hbar e^4 k}{2\epsilon^2 \epsilon_k^2 m}\left[\ln\left[1+\frac{4k^2}{q_D^2}\right] - \frac{1}{1+q_D^2/4k^2}\right] , \qquad (25)$$

where n_I is the concentration of ionized impurities. It is conceivable that, for a suitable impurity at $T \simeq 500$ K in Ge, n_I becomes sufficiently large for ionized-impurity scattering to overcome phonon scattering, and a more rapid decrease in D_+ with temperature would result. Substitution of (23) in the formal expression (19) for D_+ yields the analog of the Brooks-Herring mobility formula. However, an ionized-impurity concentration $n_I \approx 10^{19}$ cm^{-3} is required to reduce D_+ to 1 cm^2/s. We find it implausible that an ionized impurity concentration this high exists even in the near-surface region with the samples used in these studies.

Next, we estimate the effect of positron scattering from a neutral impurity or defect in the "spherical square-well" model of Bergersen *et al.*[41] We find

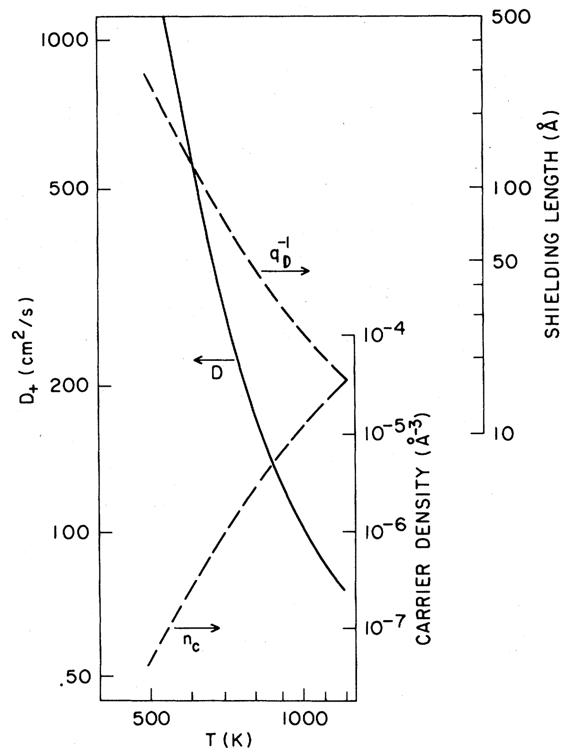

FIG. 6. Diffusion constant resulting from positron-carrier scattering in Ge. Also shown are the Debye shielding length q_D^{-1} and the thermally generated carrier density n_c (Ref. 56).

$$\tau_k^{-1} = \frac{mk}{\pi\hbar^3} n_I \Omega_0^2 (\Delta V)^2 , \tag{26}$$

where ΔV is the mean potential energy change due to the impurity or defect over the cell volume of Ω_0, and n_I is the impurity or defect concentration. The use of (21) gives

$$D_+ = \frac{2}{3} \left[\frac{2\pi}{\beta} \right]^{1/2} \frac{\hbar^4}{m^{5/2} n_I \Omega_0^2 (\Delta V)^2} . \tag{27}$$

This mechanism thus results in D_+ increasing with temperature, which is incompatible with the Ge data, except possibly at the highest temperature. However, as can be seen from Fig. 6, $D \propto T^{+0.5}$ is not a good description of these data. Furthermore, a plausible value of $\Delta V \simeq 1$ eV and the requirement that $D \simeq 1$ cm^2/s suggests that $n_I \approx 10^{22}$ cm^{-3} is required. This is an extremely high impurity concentration even for the near-surface region. It thus seems unlikely that neutral impurity or defect scattering is responsible for limiting the positron mobility in any of the present results.

C. Electric field effects on diffusion

In the presence of an electric field E within the sample the diffusion equation (6) becomes[28]

$$\frac{dn}{dt} = D_+ \nabla^2 n - \beta e D_+ \vec{\nabla} \cdot \vec{\epsilon} n - n/\tau . \tag{28}$$

In the limit where the field varies only slowly on the scale of variations of n, the additional term is

$$\beta e D_+ \vec{\nabla} \cdot \vec{\epsilon} n = \vec{v}_d \cdot \vec{\nabla} n , \tag{29}$$

where $\vec{v}_d = \mu \vec{\epsilon}$ is the positron-drift velocity. The drift term becomes significant when $v_d \tau \approx L_+$, so fields of order

$$| \vec{\epsilon}_0 | = k_B T / e L_+ \tag{30}$$

seriously inhibit or enhance positron motion, depending on their direction. For a positron of $D_+ \approx 1$ cm^2/s and $\tau \simeq 220$ ps we have $L_+ \approx 1500$ Å, giving $| \vec{\epsilon}_0 | \simeq 1700$ V/cm at 300 K. This is a rather large field, requiring low conductivity to maintain, and also one that corresponds to a surface charge density on Ge of $\approx 5 \times 10^{-9}$ C/cm^2, or about one electronic charge per 10^5 surface atoms. We are not aware of any evidence that the Ge surface tends to have such an excess of electrons or holes in surface states. The Brookhaven slow-positron-bean current is presently $\approx 10^{13}$ A, so charging of this magnitude by the beam is, in principle, achievable, but since the highest resistivity of any sample used was 2×10^7 Ω cm,[29] it is highly unlikely. It appears that the only way in which electric fields could seriously affect the positron motion is through scattering or trapping by charges in the interior of the sample, as discussed in Sec. V A.

D. Diffusion of excitations

As the positron thermalizes it deposits its initial energy E in a short time within a rather localized region of the crystal, giving local energy densities 0.01–10 meV/$Å^3$ or, specifically in Ge, 10–200 meV/atom. (Because of a greater $\bar{x}/E$ and slightly smaller atomic volume this energy per atom will be an order of magnitude smaller in Si.) Some of this energy is deposited initially in electron-hole pair excitations and some is converted directly into lattice vibrations. It is of interest to see if this energy can be dissipated sufficiently fast for positron diffusion to take place in this region at the sample temperature. In metals, the dissipation of energy away from a localized high-energy-density region is via the electrons[45] and occurs in ≈ 10 ps.[11]

In semiconductors, the excited carriers probably move away equally rapidly, and certainly the carrier diffusion constants are $\approx 10^2 D_+$. Because of the band gap, however, not all of the lattice energy in semiconductors is carried away by electronic excitations. The phonon diffusion constant in Ge is $D_{ph} = 0.05$ cm^2/s at 600 K, so the phonons dissipate energy more slowly than the positron diffuses. It should be noted that the phonon mean free path at this temperature is ≈ 150 Å.

One possible effect of this local heating is that positron diffusion occurs at a local temperature higher than the lattice temperature, so that D_+ appears almost independent of the sample temperature at low sample temperatures. Another effect is the potential effect on the positron motion of the "wind" of excitations flowing to cooler regions. A third effect involves local inhomogeneities in sample temperature. Most of the energy is deposited between the surface and the positron, and a positron in a temperature gradient $\partial T / \partial x$ experiences a driving force $E_1 (\partial T / \partial x)(\partial \ln V / \partial T)$ where $\partial \ln V / \partial T \approx 10^{-5}$ K^{-1}. If, in Ge, $E_1 \simeq 20$ eV and $\partial T / \partial x \simeq 0.1$ K/Å, we find a driving force of 2 keV/cm, comparable to the critical value $| \vec{\epsilon}_0 |$ of Sec. V C.

To estimate the sustainable temperature gradient we consider a sphere of radius 50 Å in which the lattice is initially heated to 100 meV/atom, or 400 K. Within the positron lifetime, we suppose that this radius expands to $(2 D_{ph} \tau)^{1/2} \simeq 500$ Å, and thus the final temperature is $\approx (400$ K$)/10^3 = 0.4$ K, giving a final temperature gradient $\approx 10^{-3}$ K/Å. This rough estimate indicates that the resulting strain field does not provide a very significant driving force on the positron.

E. Strong positron-phonon—coupling effects

The original hypothesis advanced by Jorch *et al.*[10] to explain the Ge data was metastable self-trapping of the positron. The positron was postulated to be free at low temperatures (< 500 K) and then to be thermally excited (by 900 K) into a metastable, but still somewhat mobile, quasiparticle state consisting of a positron surrounded by a lattice distortion. It is not, in fact, clear why the self-trapped state is not the positron ground state in Ge and Si, since the deformation-potential constants exceed the estimated threshold for self-trapping.[46,47] (Those estimates, however, give a lower bound to the self-trapping threshold.)

A self-trapped particle, or small polaron, is expected to have low mobility. There is at present some uncertainty

about the temperature dependence of D_+ that would be anticipated, since theory and possible observations of quantum diffusion disagree.[48] However, the maximum diffusion constant expected can be estimated from $D = wa^2/6$, where the maximum jump rate w cannot exceed a typical phonon frequency ($\approx 10^{13}$ Hz) if lattice relaxation is to occur, and the jump length a is not more than the <3-Å interatomic separation. The measured values of D_+ in Ge appreciably exceed this upper limit of 1×10^{-3} cm^2/s. Presumably, a metastably self-trapped positron would also exhibit low mobility, and one might anticipate a fairly large lifetime change at the temperature where self-trapping occurs. No large change has been observed; only a shift of a few picoseconds has been identified. Recently, some doubt has been cast on the possibility of metastable self-trapping, since De Raedt and Lagendijk[49] report a calculation of the small-polaron free energy which shows no temperature dependence of the critical coupling strength.

Another possibility is that there is a time delay for stable self-trapping of positrons in Ge. The dynamics of self-trapping may involve a fluctuation in the medium which exceeds some critical amplitude.[50-52] The probability of a suitable lattice distortion increases with temperature, and one hypothesis is that in Ge at $T > 500$ K a decreasing time delay for positron self-trapping increases the self-trapping rate to a value approaching the annihilation rate. Browne and Stoneham[52] discuss models of this critical strain fluctuation. To obtain a simple qualitative description, we suppose that, at the high temperatures of interest here, the atoms vibrate essentially as independent classical oscillators. The probability[52] $P(x > x_c)$ that the displacement x of a classical oscillator exceeds a critical displacement x_c is $P(x > x_c) = \mathrm{erfc}(\sqrt{\beta\epsilon_c})$, where $\epsilon_c = \frac{1}{2} m\omega^2 x_c^2$ for a mass m oscillating with frequency ω. If P is small, i.e., $\epsilon_c \gg k_B T$, as expected for only partial positron self-trapping, the complementary error function can be expanded to give a self-trapping rate proportional to $P \propto T^{1/2} e^{-\beta\epsilon_c}$. This, aside from the slowly varying $T^{1/2}$ factor, is the form used in the usual analysis of positron trapping at thermally generated defects. That analysis[29] gives a reasonable, although not perfect, fit to the present Ge data with an activation energy $\epsilon_c \simeq 0.3$ eV (Sec. V F). Of course, an apprecable lifetime change and a low mobility would still be expected for the self-trapped species.

A third conjecture which involves positron-phonon—coupling effects beyond the conventional weak-scattering limit is related to that invoked by Seager and Emin[53] as a possible explanation for the anomalous high-temperature decrease in the electronic Hall mobility of alkali halides. At nonzero temperature some particle localization can be achieved at zero-energy cost by forming a thermal wave packet. Thus, a net energy gain may result by allowing a lattice distortion to form about this wave packet. If this happens, the carrier will tend to carry this slight lattice distortion with it as it moves, leading to an effective mass somewhat greater than the bare mass. The thermal wave packet becomes more localized as the temperature increases, so the lattice distortion may become more pronounced, increasing the effective mass.

To estimate the possible effect on the mobility we follow Seager and Emin[53] in using the bandwidth renormalization expression of small-polaron theory. The bandwidth is narrowed by a factor[54]

$$Z \simeq \exp\left[-\frac{(E_1')^2}{B}\frac{R^2}{6s^2\beta}\left[\frac{m}{\pi\beta}\right]^{3/2}\right] \tag{31}$$

for coupling to acoustic phonons, where B is the bulk modulus, s is the sound velocity, and R is the jump length, taken to be approximately equal to the interatomic separation. Since the acoustic-phonon-limited diffusion constant resulting from (11) and (22) is proportional to $m^{-5/2}$, we show, as the dashed curve in Fig. 5, the result of scaling that diffusion constant by $Z^{5/2}$. The deformation-potential constant $E_1' \simeq 1.5$ eV used to evaluate Z has been chosen to roughly reproduce the positron data of Fig. 5, and is considerably smaller than the value $E_1 \simeq 20$ eV used previously. However, we note that the small-polaron Hamiltonian omits phonon-assisted hopping terms, and thus (31) probably overestimates localization effects. Hence, fitting (31) should yield $E_1' < E_1$, and thus this value may not be implausible. However, confirmation—or otherwise—must await a proper theoretical treatment, and that is not yet available.

F. Defect trapping

If defects which trap positrons are present in the sample the time τ for which the positron diffuses, as used in (9), is no longer just the inverse of the bulk annihilation rate τ_B. It also depends on the trapping rate κ_T, and is given approximately by[33]

$$\tau^{-1} = \tau_B^{-1} + \kappa_T . \tag{32}$$

If the defect profile is nonuniform in the region accessible to the positron, the positron diffusion length is no longer independent of E, as required by the model. Since we have assumed a nearly constant value for τ, trapping effects would be directly reflected in our D_+ values.

A trapping-model analysis of the Ge data suggests[29] that the decrease in D_+ above 500 K is not due to trapping at thermally generated vacancies since a formation enthalpy of ≈ 0.3 eV, in disagreement with the generally accepted 2.7 eV, would be required. Positron experiments which sample the bulk[14,42] have shown an insensitivity to both sample temperature and doping levels. We are forced to conclude that defect trapping cannot explain the temperature dependence of the Ge data.[55]

VI. CONCLUSIONS

We have experimentally studied the motion of positrons in the near-surface region of Ge from 300 to 1020 K. Our studies, which are not limited to low temperatures as are electron- and hole-mobility experiments, exhibit behavior which is not consistent with conventional understanding of electron and hole mobilities in the elemental semiconductors. Specifically, there is a temperature-dependent mobility-limiting process which is not understood, and of the possible origins of this process which we have considered only some form of a strong positron-

phonon—coupling effect appears to survive initial scrutiny.

The positron probes semiconductors as a charge carrier that not only responds to parts-per-million defect concentrations (as in metals), but also shows strong nontrapping interactions with the material. As our understanding of these interactions grows, the slow-positron-beam techniques will be used to investigate semiconductor structures such as Schottky-barrier devices, and to elucidate effects such as near-surface carrier motion and hole traps at interfaces.

ACKNOWLEDGMENTS

The authors wish to acknowledge P. J. Schultz for useful help during some of these measurements and H. W. Kraner for supplying some of the Ge samples. Useful discussions with I. K. MacKenzie and D. Emin are also asknowledged. Work performed at Brookhaven National Laboratory was supported by the Division of Materials Sciences, U.S. Department of Energy, under Contract No. DE-AC02-76CH00016.

APPENDIX A: POSITRON THERMALIZATION IN Ge AND Si

An estimate of the thermalization time t_{th} for positrons in a semiconductor can be found from the mean rate of energy loss to phonons, since the time to slow to the band-gap energy E_g by electron excitations is short in comparison with the time to slow from E_g to the sample temperature. The rate of positron energy loss by phonon emission is[12]

$$-\frac{d\epsilon}{dt}=\frac{2}{C}\epsilon^{3/2}, \tag{A1}$$

where

$$C=\frac{\pi h^4 \rho}{\sqrt{2}m^{5/2}E_1^2} \tag{A2}$$

if only deformation-potential coupling to longitudinal-acoustic phonons is considered. The optical-phonon coupling constant E_1^{opt} for positrons in Ge and Si is not yet known, but omission of optical-phonon coupling can only produce an overestimate of t_{th}.

Integration of (A1) gives

$$t_f-t_i=C(\epsilon_f^{-1/2}-\epsilon_i^{-1/2}) \tag{A3}$$

for the time to slow from an initial energy ϵ_i to a final energy ϵ_f. For $\epsilon_i=E_g$ (0.7 eV in Ge and 1.1 eV in Si) and ϵ_f a thermal energy, $\epsilon_i^{-1/2} \ll \epsilon_f^{-1/2}$ and

$$t_{\text{th}} \simeq C\epsilon_f^{-1/2}. \tag{A4}$$

TABLE II. Positron thermalization times $t_{\text{th}}=C(k_BT)^{-1/2}$ in Ge and Si.

	E_1 (eV)	$Ck_B^{-1/2}$ ($\text{K}^{1/2}$ s)	t_{th} (ps) to 300 K	t_{th} (ps) to 10 K
Ge	20	4.8×10^{-11}	3	15
Si	13	5.0×10^{-11}	3	15

The values of Table II indicate that positrons in both Ge and Si thermalize to 300 K in less than 10 ps.

APPENDIX B: POSITRON-CARRIER SCATTERING

In this simplified model we consider scattering of a positron of mass $m=m_e$ from electrons and holes of the same mass and having parabolic dispersion relations $\epsilon_k=h^2k^2/2m$. The total thermally generated density of both kinds of carriers at temperatures T will be written $n_c(T)$. The law of mass action gives

$$n_c=8\left[\frac{m}{2\pi\beta h^2}\right]^{3/2}e^{-\beta E_g/2} \tag{B1}$$

for an intrinsic semiconductor, although in our numerical estimates we have used experimental values[56] of n_c for intrinsic Ge.

The rate at which positrons of wave vector $\vec{k}$ are scattered by carriers in thermal equilibrium into states of wave vector $\vec{k}+\vec{q}$ is

$$w_{\vec{k}+\vec{q},\vec{k}}=\frac{2\pi}{\Omega^2}n_c\,|v(q)|^2 \times\sum_{\vec{k}'}\left[\frac{2\beta\pi}{m}\right]^{3/2}e^{-\beta\epsilon_{\vec{k}'}} \times\delta(\epsilon_{\vec{k}+\vec{q}}+\epsilon_{\vec{k}'-\vec{q}}-\epsilon_{\vec{k}}-\epsilon_{\vec{k}'}) \tag{B2}$$

($\hbar=1$), where

$$v(q)=-\frac{4\pi e^2}{\epsilon(q^2+q_D^2)} \tag{B3}$$

is the shielded potential and Ω is the volume. The ratio of the reciprocal shielding length q_D (24) to the positron thermal wave vector $k_{\text{th}}=(3mk_BT)^{1/2}$ is given by

$$\frac{q_D^2}{k_{\text{th}}^2}=\frac{16\pi}{3\epsilon}\left[\frac{\beta e^2}{2a_0}\right]^2 n_c a_0^3, \tag{B4}$$

where a_0 is the Bohr radius. Since, by 1000 K, q_D/k_{th} only rises to ≈ 0.2 in Ge, we take the scattering to be elastic, and find

$$\tau_k^{-1}=\frac{e^2q_D^2}{4\pi\epsilon}\frac{(2\beta\pi/m)^{1/2}}{\beta\epsilon_k} \times\int_0^\infty\frac{x^3dx}{(x^2+\beta q_D^2/2m)^2} \times\int_0^\infty d\mu(1-\mu^2)e^{-(x-\mu\sqrt{\beta\epsilon_k})^2}. \tag{B5}$$

The positron diffusion constant which results from the use of this expression for the relaxation rate in (21) is shown in Fig. 6. There is a strong temperature dependence ($\xi\simeq4$ for $500<T<1000$ K), but the values of D_+ remain more than an order of magnitude larger than the measured values over the entire temperature range.

*Present address: Department of Physics, Royal Roads Military College, FMO, Victoria, British Columbia, Canada V0S 1B0.
†Present address: Department of Physics, Queen's University, Kingston, Ontario, Canada K7L 3N6.

[1] C. Canali, C. Jacoboni, F. Nava, G. Ottaviani, and A. Alberigi-Quaranta, Phys. Rev. B **12**, 2265 (1975).
[2] G. Ottaviani, L. Reggiani, C. Canaldi, F. Nava, and A. Alberigi-Quaranta, Phys. Rev. B **12**, 3318 (1975).
[3] C. Jacoboni, F. Nava, C. Canali, and G. Ottaviani, Phys. Rev. B **24**, 1014 (1981).
[4] L. Reggiani, C. Canali, F. Nava, and G. Ottaviani, Phys. Rev. B **16**, 2781 (1977).
[5] L. Reggiani, S. Bosi, C. Canali, F. Nava, and S. F. Kozlov, Phys. Rev. B **23**, 3050 (1981).
[6] Attempts to measure positron mobility in diamond have only established upper limits; see G. Lang and S. DeBenedetti, Phys. Rev. **108**, 914 (1957); O. Sueoka and S. Koide, J. Phys. Soc. Jpn. **41**, 116 (1976).
[7] A. P. Mills, Jr. and L. N. Pfeiffer, Phys. Rev. Lett. **36**, 1389 (1976).
[8] A. P. Mills, Jr. and L. Pfeiffer, Phys. Lett. **63A**, 118 (1977).
[9] A. P. Mills, Jr., in *Positron Solid State Physics,* edited by W. Brandt and A. Dupasquier (North-Holland, Amsterdam, 1983).
[10] H. H. Jorch, K. G. Lynn, and I. K. MacKenzie, Phys. Rev. Lett. **47**, 362 (1981).
[11] P. Kubica and A. T. Stewart, Phys. Rev. Lett. **34**, 852 (1975).
[12] A. Perkins and J. P. Carbotte, Phys. Rev. B **1**, 101 (1970).
[13] R. M. Nieminen and J. Oliva, Phys. Rev. B **22**, 2226 (1980).
[14] M. A. Shulman, G. M. Beardsley, and S. Berko, Appl. Phys. **5**, 367 (1975).
[15] H. J. Mikeska, Phys. Lett. **24A**, 402 (1967); Z. Phys. **232**, 159 (1970).
[16] B. Bergersen and E. Pajanne, Phys. Rev. B **3**, 1588 (1971).
[17] The stopping profile is usually normalized to unity.
[18] A. P. Mills, Jr. and R. J. Wilson, Phys. Rev. A **26**, 490 (1982).
[19] A. P. Mills, Jr., Phys. Rev. Lett. **41**, 1828 (1978).
[20] K. G. Lynn and D. O. Welch, Phys. Rev. B **22**, 99 (1980).
[21] R. M. Nieminen and M. J. Manninen, in *Positrons in Solids,* edited by P. Hautojärvi (Springer, New York, 1979).
[22] K. G. Lynn, Phys. Rev. Lett. **43**, 391 (1979).
[23] K. G. Lynn, J. Phys. C **12**, L435 (1979).
[24] A. P. Mills, Jr., Phys. Rev. Lett. **46**, 717 (1981).
[25] A. P. Mills, Jr., P. M. Platzman, and B. L. Brown, Phys. Rev. Lett. **41**, 1076 (1978).
[26] D. A. Fischer, K. G. Lynn, and W. E. Frieze, Phys. Rev. Lett. **50**, 1149 (1983).
[27] A. P. Mills, Jr. and P. M. Platzman, Solid State Commun. **35**, 321 (1980).
[28] A. P. Mills, Jr. and C. A. Murray, Appl. Phys. **21**, 323 (1980).
[29] H. H. Jorch, Ph.D. thesis, University of Guelph, 1981.
[30] K. G. Lynn and H. Lutz, Phys. Rev. B **22**, 4143 (1980).
[31] S. Valkealahti and R. M. Nieminen, Appl. Phys. A **32**, 95 (1983).
[32] K. G. Lynn and H. Lutz, Rev. Sci. Instrum. **51**, 977 (1980).
[33] P. J. Schultz, K. G. Lynn, R. N. West, C. L. Snead, Jr., I. K. MacKenzie, and R. W. Hendricks, Phys. Rev. B **25**, 3637 (1982).
[34] S. Dannefaer, J. Phys. C **15**, 599 (1982).
[35] P. J. Schultz and I. K. MacKenzie, in *Positron Annihilation,* edited by P. G. Coleman, S. C. Sharma, and L. M. Diana (North-Holland, Amsterdam, 1982), p. 640.
[36] K. G. Lynn, in *Positron Solid State Physics,* Ref. 9.
[37] W. A. Harrison, Phys. Rev. **104**, 1281 (1956).
[38] E. M. Conwell, in *High Field Transport in Semiconductors,* Supplement 9 of *Solid State Physics* (Academic, New York, 1967).
[39] T. McMullen, in *Positron Annihilation,* Ref. 35.
[40] This is weaker than the $\alpha \simeq 2-3$ dependence given in Ref. 10, which was the result of a preliminary analysis.
[41] B. Bergersen, E. Pajanne, P. Kubica, M. J. Stott, and C. H. Hodges, Solid State Commun. **15**, 1377 (1974).
[42] S. Tanigawa, K. Hinode, R. Nagai, and M. Doyama, Appl. Phys. **18**, 81 (1979).
[43] M. Dorikens, C. Dauwe, and L. Dorikens-VanPraet, Appl. Phys. **4**, 271 (1974); W. Fuhs, U. Holzhauer, and F. W. Richter, *ibid.* **22**, 415 (1980).
[44] H. Weisberg and S. Berko, Phys. Rev. **154**, 249 (1967).
[45] G. J. Dienes and G. H. Vineyard, *Radiation Effects in Solids,* (Interscience, New York, 1957).
[46] C. H. Hodges and H. Trinkhaus, Solid State Commun. **18**, 1857 (1976).
[47] C. H. Leung, T. McMullen, and M. J. Stott, J. Phys. F **6**, 1063 (1976).
[48] K. W. Kehr, D. Richter, J. M. Welter, O. Hartmann, E. Karlsson, L. O. Nordlin, T. O. Niinikoski, and A. Yaouanc, Phys. Rev. B **26**, 567 (1982).
[49] H. De Raedt and A. Lagendijk, Phys. Rev. Lett. **49**, 1522 (1982).
[50] N. F. Mott and A. M. Stoneham, J. Phys. C **10**, 3391 (1977).
[51] D. Emin, Hyperfine Interact. **8**, 515 (1981).
[52] A. E. Browne and A. M. Stoneham, J. Phys. C **15**, 2709 (1982).
[53] C. H. Seager and D. Emin, Phys. Rev. B **2**, 3421 (1970).
[54] T. McMullen and B. Bergersen, Solid State Commun. **28**, 31 (1978).
[55] The two data points in Ref. 19 for Ge are in agreement with our data.
[56] F. J. Morin and A. P. Maita, Phys. Rev. **94**, 1525 (1954).